Nano-enabled approaches to chemical imaging in biosystems

Scott T. Retterer[1, 2], Jennifer L. Morrell-Falvey[1], Mitchel J. Doktycz[1,2]

[1]Biosciences Division and [2] Center for Nanophase Materials Science, Oak Ridge National Laboratory, Oak Ridge TN, USA

rettererst@ornl.gov, morrelljl1@ornl.gov, doktyczmj@ornl.gov

CORRESPONDING AUTHOR

Mitchel Doktycz

Oak Ridge National Laboratory

P.O Box 2008

Oak Ridge, Tennessee 37831

865-574-6204

RUNNING TITLE: Nano-enabled chemical imaging

KEYWORDS

Nanoparticles, microfluidics, chemical imaging, multimodal imaging, metamaterials, super resolution

ABSTRACT

Understanding and predicting how biosystems function requires knowledge about the dynamic, physico-chemical environments with which they interact and alter by their presence. Yet, identifying specific components, tracking the dynamics of the system, and monitoring local environmental conditions without disrupting biosystem function present significant challenges for analytical measurements. Nanomaterials, by their very size and nature, can act as probes and interfaces to biosystems and offer solutions to some of these challenges. At the nanoscale, material properties emerge that can be exploited for localizing biomolecules and making chemical measurements at cellular and sub-cellular scales. Here, we review advances in chemical imaging enabled by nanoscale structures, in the use of nanoparticles as chemical and environmental probes, and in the development of micro- and nanoscale fluidic devices to define and manipulate local environments and facilitate chemical measurements of complex biosystems. Integration of these nano-enabled methods will lead to an unprecedented understanding of biosystem function.

1. INTRODUCTION

Biological systems consist of thousands of interacting molecular components within the confines of a cell that is only microns in size. Identifying the specific components that are present, monitoring the local physical and environmental conditions, and tracking the dynamic, spatial orchestration of its interacting systems present a profound challenge for analytical measurements. Ideally, such measurements would observe the components of living systems in a minimally perturbing manner, without the use of extrinsic labels. However, the diverse

components that comprise the biological cell make comprehensive identification and localization of chemical information extremely difficult. The typical cell contains thousands of genes, and tracking the production and location of gene products is critical to functional insights. Here, genetically incorporated labels have greatly facilitated monitoring gene expression and protein localization (1). In contrast, the small size of typical metabolites prevents simple labeling with extrinsic or genetically encoded tags. Microbial cells may produce thousands of distinct small molecules, while higher order organisms can generate orders of magnitude more (2). However, simultaneously tracking the location and concentration of more than just a few proteins or metabolites quickly becomes intractable by existing techniques.

Various microscopies have been essential to resolving functional aspects of biological systems. Often, nanotechnologies are integral to these tools or have led to entirely new approaches to imaging biological systems. Perhaps the pioneering example is scanning probe microscopy (SPM). Since its introduction more than three decades ago, SPM was immediately applied to biological studies and has spun into an extensive array of nanoscale chemical and physical imaging techniques (3). Similarly, nanomaterial labels expand the range of detection modalities and facilitate sensitive measurements. Nanomaterials, and the nanometer length scale in general, cover a size range that bestows useful benefits for imaging at the molecular and cellular levels. At the nanoscale, material properties emerge that lead to concentration of electromagnetic fields, useful mechanisms for sensing, and amplification of signals emanating from the single molecule level. These properties can be readily exploited for localizing biological species and for making chemical measurements at cellular and sub-cellular scales. Further, the working levels of biological systems overlap the very size of nanostructures making them effective probes and interfaces to biological systems. Highly defined spatial and temporal

mapping of cellular components becomes possible as the measurement probe reduces in size. This can facilitate multimodal imaging where spatial and temporal information are mapped with chemical information.

Diverse imaging technologies attempt to address chemical identification needs and typically employ some form of electromagnetic energy to probe biological materials. Spatially dependent chemical information can be obtained using near infrared, Raman, electron, x-ray and mass spectrometry-based techniques (4). For many of these techniques, the experimental approach involves fixing samples and carrying out characterization in a low-pressure environment. Nevertheless, spatially resolved chemical information can be obtained at defined time points. Chemical imaging tools that employ mass spectrometry are growing in popularity. This appeal is due to the technique's ability to sensitively detect a broad range of chemical species without the need for labeling (5). Some imaging mass spectrometry techniques are implemented in vacuum and can be destructive, precluding analyses on living systems. However, sampling and ionization approaches that are minimally perturbing and function under ambient conditions are emerging. Mass spectrometry-based chemical imaging methods have been reviewed recently and will not be covered here (5-7).

In general, chemical imaging and imaging enabled by nanoscale structures, or "nano-enabled" imaging, can take different forms (Figure 1). The approach of nano-enabled chemical imaging is emerging and is poised to create a powerful arsenal of tools for attacking the problem of understanding biological function across complex systems and multiple length scales. Advances in the founding technology of scanning probe microscopy and its application to biological systems are well described and will not be discussed here (8, 9). Here, we focus specifically on tools that use nanomaterials and nanostructured surfaces to facilitate live

biological imaging, where the dynamics of these systems can be observed and measured. Though biological systems function across molecular and ecosystem scales, we focus specifically on those tools used for measurements across the molecular, cellular, and multi-cellular dimensions. Emerging optical imaging technologies that exploit nanofabricated structures will be highlighted. Optical imaging has long been integral to gaining a physical and chemical understanding of biological systems. Various nano-enabled optical imaging technologies are breaking diffraction barrier limits and are poised to increase the accessibility of super-resolution techniques. Also highlighted will be recent advances in nanomaterial-based contrast agents. A variety of nanoparticle structures have been developed for detecting chemical species and environmental conditions. These materials can be delivered to specific locations or broadly sample a system and its environment. Controlling this environment and facilitating sensitive chemical measurements through development and application of multiscale fluidic imaging environments is a final focus topic. Micro- and nanofabrication techniques are being used to define the imaging environment and to create nanostructures that can enhance spatial resolution, increase the sensitivity of chemical measurements, or activate chemical processes. A subset of these nanostructured surfaces includes nanofluidic-based elements, which can be used for routing and sensing of chemical information. Finally, we conclude with an outlook on these nano-enabled technologies and how they can be combined to allow an unprecedented understanding of biological systems.

2. ENABLING OPTICAL IMAGING

Optical imaging techniques are a standard tool for characterizing physical architecture and chemical composition. However, the spatial resolution of conventional optical microscopy is diffraction limited and related to the wavelength of light that is employed and the refractive

index of the medium. Breaking this barrier can transform our understanding of biological systems as demonstrated by the recent accessibility of various super resolution microscopies (10). Typically, these techniques employ novel fluorescence excitation and sampling schemes to improve resolution. Alternatively, nanostructured materials can be employed to enhance the resolution of optical imaging. These approaches leverage the small size and photonic properties of a nanostructured material to access the non-propagating, near-field information that results from light-matter interactions. Projecting this near field information into the far field has been technically challenging, but is increasingly giving way due to advances in nanofabrication. Highlights of these emerging approaches are described below.

2.1 Accessing near-field information

The scanning near-field microscope (SNOM, or near-field scanning optical microscope, NSOM) is an early example of the use of nanostructured materials for super resolution imaging. In SNOM, the information from the evanescent field is translated into the far field by placing a sharp probe close to the sample, typically at nanometer scale distances. Commonly, the probe is a sub-wavelength scale aperture that can deliver and/or receive light energy depending on the excitation scheme employed. Alternatively, far field light can be used to focus energy at the tip of the probe (tip-enhanced near-field optical microscopy). In either case, the localized interaction of energy with the surface results in propagating radiation that is detected and translated into an image by raster scanning the position of the tip relative to the surface. The technique has matured over the past several decades and numerous reviews detail the various configurations, operational modes and applications of this powerful microscopy technique (11-13). Particularly exciting for chemical imaging has been tip enhanced near-field optical microscopy, which couples the excitation light at the tip to enhance Raman and fluorescence signals (14, 15).

Other approaches to accessing near-field optical information through nanostructured materials are emerging. When compared to SNOM, many of these microscopy applications are in an early stage of development but offer exciting possibilities for facilitating the imaging of biological systems. The ability to fabricate and pattern nanomaterials allows for the control of light in unprecedented ways (16). Designed "metamaterials" can allow optical designs that extend near field information into the far field (17-19). These approaches leverage the photonic properties of nanostructured materials to view subwavelength scale information. Pioneering experimental efforts have supported the predicted benefits of creating metamaterials with a negative index of refraction (20). For example, superlenses created from metamaterials have demonstrated the ability to resolve subwavelength features by propagating and enhancing evanescent waves through a stack of nanoscale materials (21, 22). Metamaterials prepared from aligned nanowire arrays are also being considered for breaking the diffraction barrier (23). Conductance of near field information, either through excitation and guiding of surface plasmon polaritons (24) or by the transport of evanescent waves through the metamaterial (25) have been demonstrated. These metamaterial-based lenses are still challenging to fabricate and employ but offer a promising route to imaging below the diffraction limit.

A practical approach to enhancing resolution uses solid immersion lenses (SILs) (26). Conventionally, SILs allow for improved imaging resolution by increasing the refractive index of the medium, and hence the numerical aperture, as with liquid immersion. A nanoscale SIL (nSIL), where the lens is sub-wavelength in size, has the added benefit of focusing the near field. Innovative nanofabrication approaches have led to the preparation of nSILs that result in resolution improvements. For example, calix(4)hydroquinone can self-assemble into plano-spherical lenses that allow imaging at the nanoscale (27). Recently, Fan and colleagues have

shown that TiO_2 nanoparticles self-assemble into lens shaped structures after spraying and drying the particles onto a surface (28). Direct fabrication of lens shaped structures has been demonstrated by thermal reflowing of electron-beam defined posts, which can be further replicated by soft lithography (29). Other nSIL fabrication techniques include dip pen nanolithography (30) and stamping from nanopillars (31). These structures all result in feature resolution well below the diffraction limit. In practice, the nSIL is in intimate contact with the object to be imaged and the field of view is limited to the central portion of the face of the lens. SIL structures are beginning to be applied to biological samples (32).

Super resolution lensing capabilities are also possible using sphere-shaped structures. Microspheres, on the order of 2 – 9 μm in diameter, can act as far-field superlenses (33). Even larger diameter spheres, up to a few hundred microns also provide super resolution when immersed in liquids or solids (34). In the transverse direction, rod shaped structures can also enhance the resolution of imaging, albeit with a magnified field of view along the length of the rod (35, 36). The origin of the enhancement in microsphere-based imaging is uncertain, and can stem from the presence of high refractive index materials, an enhanced near field and "photonic nanojet" phenomena (37-39). Nevertheless, the accessibility and simplicity of the approach make it a promising tool for cost effective nanoscopy. For example, microspheres are easily employed with wide field microscopes, and even greater resolution is possible when combined with a confocal laser scanning system (40).

When using microspheres, numerous techniques for increasing the field of view and ease of use are emerging. A single microsphere provides a field of view on the order of a few microns. The use of multiple microspheres or scanned systems can greatly increase information content. One promising approach embeds an array of microspheres into a coverslip coated with

polydimethylsiloxane (38, 41, 42). This straightforward use of conventional imaging materials allows prefabrication and combines the spheres with a medium of appropriate refractive index contrast. Random and directed microsphere scanning methods are also being advanced. Initial efforts used a micropipette to trap a microsphere and subsequently directed the sphere to the desired field of view (43). Other approaches have used microspheres attached to the end of the cantilever of the scanning probe microscope (44, 45). This latter approach permits surface sensing for precise positioning of the bead above the sample and biological imaging (Figure 2a). These directed scanning efforts are complemented by untethered approaches. Chemically powered microbeads, where a portion of the bead surface is coated with a magnetic/catalytic patch, can be used to directionally traverse the microsphere across a sample (46). Here, the random sampling method simplifies instrumentation requirements while the use of multiple microbeads facilitates rapid image collection. Random position scanning techniques, based on diffusionally transported nanoparticles that collect near field information, have also been described and present another approach for collecting images over a large field of view (47). Finally, the simplicity of the microsphere imaging technique has led to rapid demonstration of its applicability to biological imaging. Molecular and cellular characterizations along with its compatibility with common fluorescent labeling has been demonstrated for a number of biological structures (41, 44, 48, 49).

2.2 Super-oscillatory lenses

As described, microspheres, microwires and nSILs can be integrated directly with samples and approaches to expanding their field of view are being developed. Nevertheless, near intimate contact of the nanostructured material with the material being image is required. This can potentially interfere with the sample being studied and may limit the collection of dynamic

information. Super-oscillatory lenses are an emerging class of nanostructured materials that are poised to overcome these limitations while also providing super resolution. A super-oscillatory lens uses a nanostructured mask to diffract light into a subwavelength scale spot at a relatively long working distance, tens of microns (Figure 2b). The lens can be implemented in a scanning mode to produce a large field of view, like a conventional laser scanning confocal microscope (50). Variations of the technology allow sub-diffraction imaging resolution without scanning at even longer working distances (51). Further, a recent demonstration has shown that super resolution and long working distances are possible without the need for defining sub-wavelength features in the lens (52). This can greatly simplify manufacture and adaptation of the technology.

3. NANOPARTICLES AS CHEMICAL IMAGING AGENTS

Nanoparticles have ushered in exciting possibilities for imaging-based chemical identification due to their small size – on the order of proteins – and customizable physical properties. The combinations of different sizes, shapes, compositions, and surface chemistries with which nanoparticles can be engineered, and their compatibility with conventional imaging platforms broaden their appeal and potential applications. Indeed, initial demonstrations of nano-enabled super-resolution imaging technologies employed nanoparticle labels to demonstrate resolution and sensitivity (32) First discovered in the early 1980s (53), colloidal semiconductor nanocrystals (quantum dots) have found a long-standing use for localizing biomolecules and probing cellular functions. In part, these applications have been driven by shortcomings associated with fluorescent dyes and genetically engineered fluorescent proteins, which are easily photobleached and have limited multiplexing capabilities due to their broad excitation and emission spectral profiles. Semiconductor quantum dots, on the other hand, are

highly resistant to photobleaching with broad excitation spectra and narrow fluorescent emission spectra. The breakthrough for biological imaging came with the ability to modify the surface of quantum dots to improve biocompatibility and directly target select biomolecules (54-57). Quantum dots conjugated to antibodies, ligands, small molecules, and nucleic acids have allowed dynamic localization of many cellular components and driven insights into cellular functions (58, 59).

Advances in the use of nanoparticles as contrast agents include facilitating their biocompatibility and targeting abilities. One drawback of using semiconductor quantum dots is that the presence of cadmium or other heavy metals in the core can cause cellular toxicity and environmental concerns. Recently, nanoscale carbon particles (carbon dots, C-dots) have been described that have spectral properties similar to quantum dots (60). One of the first examples of in vivo imaging using carbon dots involved injecting carbon dots passivated with PEG into mice and performing whole body imaging to demonstrate sustained fluorescence and non-toxicity of the nanoparticles (61). In addition, new synthesis methods have been described in which fluorescent dyes can be incorporated directly into the volume of silica nanoparticles, producing stably fluorescent and/or radiolabeled nanoparticles that can be surface functionalized (62). These methods have been further expanded to facilitate the synthesis of volume labeled core-shell particles (63).

The ability to deliver nanoparticles to cells and subcellular locations and subsequently use those particles to detect local changes in the chemical environment offers an exciting opportunity for their use. In eukaryotic cells, nanoparticles can be modified with ligands that target surface receptors or alter protein adsorption in order to alter their uptake by endocytosis (64). For example, lysosomal pH was monitored using a fluorescent silicon nanodot conjugated

to a pH-sensitive FITC-tagged aptamer (65). The aptamer targets nucleolin, a protein enriched in the membrane of cancer cells. Thus, the resulting nanosensor is selectively taken up by cancer cells and can be used to monitor lysosomal pH in these cells as demonstrated using the breast cancer cell line MCF-7 (65). In general, much of the research involving nanoparticles and bacteria has focused on the use of nanoparticles as antimicrobial agents (66) or in diagnostic assays (67). Delivery of nanoparticles inside bacteria for functional studies is hindered, at least in part, by transport across the cell wall, although uptake of nanoparticles functionalized with adenine has been demonstrated (68).

Another chemical imaging application of nanoparticles is for facilitating Raman microscopy. Raman spectroscopy is a powerful chemical analysis tool but is limited by the fact that Raman signals are inherently weak (69). However, the signals can be amplified by a number of techniques including the use surface enhanced Raman spectroscopy (SERS) in which the molecular signal is amplified when the molecule of interest is in close proximity to a surface enhancing feature (70-72). Gold or silver nanoparticles are commonly used as their optical properties can be modulated by controlling their size and shape, thereby facilitating SERS. This was demonstrated in biological systems by coating bacteria with silver nanoparticles for detection in drinking water (73). The ability to detect chemical signatures in microbial communities is confounded by the diversity of metabolites produced and the relatively low abundance of any given metabolite. To overcome these issues, silver nanoparticles were used as the signal enhancing agent when applied to *Pseudomonas aeruginosa* biofilms that produce the virulence factor pyocyanin, thereby allowing the distribution of pyocyanin to be mapped in the biofilm using a combination of SERS and principle component analyses (PCA) (74). A similar approach was also used to image the localization of flavins in *Pantoea* sp. YR343 in the presence

of resonantly enhanced carotenoid pigments (75). The range of surfaces that are compatible with SERS has been expanded by the introduction of the shell-isolated nanoparticle-enhanced Raman spectroscopy (SHINERS) technique, which protects the gold or silver nanoparticle core with a continuous shell of inert silica, thereby retaining the surface enhancement but reducing potential interference by the gold or silver nanoparticles on chemical processes (76). These shell-isolated nanoparticles have found a wide-range of uses in bioanalyses (77).

Beyond their use as localization probes, distributed nanoparticles can act as sentinels for chemical species and local environmental conditions. In particular, hybrid nanoparticle design and synthesis are opening new avenues for reporting on the dynamic distribution of chemical species and metabolic activity in complex biosystems. A general overview of their structure is shown in Figure 3a. For example, hybrid nanoparticles are being used to measure the distribution of metal ions in living systems. Metal ions act as cofactors in many cellular processes, including gene transcription, enzymatic reactions, and immune functions. Moreover, the presence of excess metal ions can be toxic to cells and biosystems so it is of particular interest to understand how these metals are transported and distributed over time. To this end, a copper-sensing hybrid nanoparticle was recently reported consisting of a core CdSe/ZnS quantum dot that emits red fluorescence, overlayed with a shell carbon quantum dot that emits blue fluorescence functionalized with a Cu^{2+} ion-specific compound. Upon binding of Cu^{2+} ions to the hybrid nanoparticle, the blue fluorescence of the shell particle is quenched, but the core red fluorescence is unaltered, providing a ratiometric fluorescence sensor of Cu^{2+} ions in HeLa cells(78). Similarly, a reversible ratiometric hybrid nanoparticle for copper sensing was also reported in which carbon dots were functionalized with triethylenetetramine to recognize Cu^{2+} and glutathione and demonstrated in yeast cells (79). Mercury ions were also detected in living HeLa

cells using a similar design in which the fluorescence of a dye coupled to a mercury ion recognition group was quenched upon mercury binding (80). Producing a ratiometric nanoparticle with an environmentally insensitive dye at the core allows for a dynamic readout of changing conditions, but results in a more complex synthesis procedure. A simplified synthesis approach was used to produce fluorescent carbon dots for mercury sensing that allowed detection, but not quantification, of mercury in HUVEC cells (81).

In addition to detecting the distribution of metals, hybrid nanoparticles are also being used to probe the pH of local microenvironments in complex biosystems. This was nicely demonstrated using ratiometric core-shell nanosensors to image pH in a bacterial biofilm (82). The nanosensor was designed using a pH-insensitive dye in the core and a pH-sensitive dye in the shell, allowing ratiometric quantification of local pH environments in a three-dimensional biofilm (Figure 3b). Comparisons of different sized nanoparticle sensors showed that only the smallest nanosensors (10 nm diameter) were well-distributed in the biofilm, pointing out the importance of understanding and controlling nanoparticle delivery and distribution in complex systems. Similar ratiometric hybrid nanoparticles were designed to monitor pH in lysosomes, an acidic organelle found in eukaryotic cells. Using the principle of fluorescence resonance energy transfer (FRET), a pH nanosensor was designed with a donor fluorophore in the particle core and an acceptor fluorophore on the particle surface that responds to increasing pH by a conformational change (83). This ratiometic nanoparticle sensor was demonstrated in HeLa cells in which the nanoparticle sensor localized to the lysosomes and was responsive to changes in pH induced by treatment with alkaline or acidic buffer solutions (83). Ratiometric nanosensors have also been described for monitoring the production of hydrogen peroxide (H_2O_2), a measure of oxidative stress in live cells. Unlike the previously described ratiometric chemical nanosensors

in which sensing results in fluorescence quenching, this nanosensor results in increased fluorescence upon detection of H_2O_2 production by human T lymphocyte Jurkat cells (84).

The applicability of hybrid nanoparticles as chemical sentinels in live cell imaging is rapidly maturing. The characteristic features of narrow emission spectra and chemical selectivity will likely lead to multiplexed chemical sensing of a broad range of molecular species. These efforts leverage diagnostic uses of these materials where they find application for the testing of water, food or biological materials for the presence of specific contaminants. Indeed, the synthesis and application of new nanosensors are being reported at a rapid rate, including nanosensors for detection of glucose (85), telomere DNA (86), double stranded DNA (87), cadmium ions (88), mercury and biological thiols (89, 90), spores (91), bisphenol A (92), and phenolic carbofuran (93). While the aforementioned nanosensors were designed primarily for sample testing, they are likely adaptable for chemical imaging applications in living systems.

4. MULTISCALE FLUIDIC IMAGING ENVIRONMENTS

4. 1 Chemically defined habitats

Micro- and nanofluidics have played an essential role in advancing imaging platforms and techniques that allow for active chemical interrogation of complex biological systems. In particular, platforms based on these technologies allow for control of the chemical and physical environment and facilitate chemical sampling and analysis. The reduced scales and unique laminar flow profiles that accompany microfluidic systems allow for predictable changes in, and manipulation of, the hydrodynamic, chemical, and thermal microenvironment at the cellular and sub-cellular scales (94-97). Early work in the development of soft lithography and silicone-based microfluidics in the late ‘90s and early 2000s highlighted the use of easily replicated silicone microfluidics, fluidic control elements, and optical structures created using soft lithography for

use in the culture and manipulation of living cells (98-101). The transparent nature of the fluidic elements, gas permeability, low-cost of replication, and potential for large-scale integration (101) ushered in decades of research built around the simple idea that we could learn more about biological systems by observing them in functional microscale habitats. In these habitats, the local environment could be shaped *a priori*, manipulated in real time, and multiplexed to perform hundreds of experiments simultaneously. Importantly, these experiments demonstrated the utility of microfluidics for assembling and supporting cells in both 2D and 3D culture as a means of promoting differentiation and retention of physiologically relevant phenotypes (102-105). Microfluidic culture models have had a significant impact on a broad range of research, from fundamental research in developmental biology to applied work in the fields of biological cell-based sensing and tissue engineering. The connectivity and networking of multi-chamber fluidic systems gave rise to the organ, and organism-on-chip concepts, which have opened new opportunities for experimentally validating pharmacokinetics and pharmacodynamics models of drug transport and metabolism (106-109). This work highlights the use of fluidic environments to define habitats for studies at the cellular, tissue- and organism-mimic levels. These efforts underscore the potential for characterizing complex biological systems by imaging chemical signals that link events across a broad range of system hierarchies.

In addition to biomedically focused systems, multiscale fluidic environments have been developed for investigating a range of different biosystems and environmental habitats. Indeed, multiscale fluidic habitats have been developed to address questions related to plant physiology (110-113), microbial ecology (114-116), and cross-kingdom interactions between plants and microbes (117, 118). Similarities in natural architectures led to the recognition that previous work in the study of axonal growth and development (119, 120) could inform fluidic designs for

tracking the growth and development of plant roots and fungal hyphae in response to biological, chemical signals, and topographical signals (121). The optical accessibility of microfluidic habitats combined with the capacity to shape tortuous environments and species interactions in a manner that reflects key features of natural systems allows researchers to address questions that could not be answered in natural settings.

Beyond being simple fluid conduits joined together to form more elaborate networks, microfluidic systems are being intentionally designed and chemically modified to promote interactions with biological systems. In this manner, information on the physical and chemical reactivity of biological systems can be gained. For example, cell attachment and growth can be enhanced by surface modification of planar glass, silicon or polymer substrates during microfluidic assembly, allowing control of individual cell growth and death (122), gene expression of developing micro-tissues (123), microbial cell-cell interactions and aggregation (124, 125), and interactions between different species and cell types (126, 127). In addition, microcontact printing, microstenciling, and lithographic patterning of biomolecules can be performed prior to habitat assembly. Controlling where biological elements reside within a functional fluidic system is an essential element to many of the platforms described above. This patterning or capture allows for effective multiplexing of biochemical experiments and/or biological tissue and cell culture, increasing experimental throughput by facilitating massively parallel experiments using limited amounts of reagents.

Complementing topographical and chemical modification of surfaces to control the attachment, growth and development of biological systems, physical containment and confinement of biological systems can be used to direct the growth and control communication between living systems (Figure 4). Nanoporous membranes have been created perpendicular to

the imaging plane using advanced nanofabrication processes that combine photolithography, advanced electron beam lithography, and reactive ion etching to create nanoporous environments that allow biological systems to develop in close proximity to one another, communicating chemically, but not physically (128-130). In contrast, in-situ patterning and crosslinking of materials like hydrogels and proteins have also been used to structure the local micro-environment and alter confinement (131-133). Connell et al. used 3D lithography to produce picoliter scale 'traps' from crosslinked proteins to study social interactions within bacterial communities (133). The fidelity of the process allowed the capture and perturbation of cells down to the single cell level.

Confinement and control of a biological system of interest can be combined with complex spatial and temporal gradients of nutrient and chemicals to drive or perturb biological processes (134). This can facilitate insights into how systems dynamically respond to changes in the chemical environment. The scale of conventional microfluidics allows laminar flow and diffusive mixing to effectively and predictably create chemical gradients that can be rapidly altered, and visualized within the viewing field of a conventional optical microscope. This allows one to observe the response of living systems to these spatiotemporal fluctuations and gradients. Gradients of varied complexity in composition and dynamics enable studies of phenomena such as microbial (135-138) and mammalian cell chemotaxis (139-141). In conjunction with looking at biological responses to chemoattractants, the response of living systems to hydrodynamic shear forces combined with changing chemical environments has also been applied to the study of processes involved in clot formation (142-145), and biofilm development (146-149).

4. 2 Fluidics within fluidics

The variety of fabrication techniques available for creating fluidic architectures of varying scales and intricacy also facilitates direct chemical sampling and analysis. Fluidic systems embedded within, and adjacent to, microfluidic habitats can be generated to effectively route chemicals and reagents around and across these habitats. These 'subnetworks' afford the researcher the opportunity to dose and sample the local chemical environment for both targeted system perturbations and sample analysis, 'eavesdropping' on the exchange of chemical information within the system. The use of nanostructured filters and membranes to separate fluidic environments and facilitate sampling and dosing without significantly altering the hydrodynamic profiles within adjacent microfluidic habitats is integral to this approach. Nanoporous membranes in the sample plane (130) and multilayer membrane platforms systems have been utilized to facilitate chemical exchange adjacent to living systems (150).

In the context of nano-enabled imaging, a porous (nanoporous) membrane serves multiple roles. As described above, confining the biological system of interest to specific locations within a habitat, that is providing a boundary across which nutrients are delivered and analytes are sampled, is essential. Additional functionality can be imparted to the membrane by chemical functionalization to potentially extract chemicals of interest via size, charge and chemical characteristics. Both nano- and microporous membranes, perpendicular to the plane of the sample, have been utilized for such purposes. Membranes created using a combination of conventional and advanced lithographic processes have been used to control the exchange of materials for complex biosynthetic reactions (151-155), housing growing populations of microbial populations (130, 132, 133), and development of high-throughput mammalian cell culture arrays (156).

Multilayer fluidic systems separated by both commercial and nanofabricated membranes, positioned parallel to and beneath the sample, have been used extensively in the development of microfluidics-based tissue culture and organ-on-a-chip platforms. Many of these applications adapted fabrication strategies employed in earlier work that focused on the development of microfluidics for analytical chemistry. In that work researchers used commercial membranes embedded in PDMS and PMMA to create multilayer systems for sample clean up and concentration (157-159). Combining these approaches with familiar Transwell™ plate culture techniques a host of organ-on-chip platforms have emerged that have explored multilayer cell co-culture and cell barrier properties using commercial membranes and silicone microfabricated constructs(107, 150, 160).

One of the truly exciting opportunities that has accompanied the development of these multilayered and multiscale fluidic platforms is the option to use the underlying and adjacent fluidic network as a means of sampling and monitoring the environment without physically disturbing the biological system of interest. In the work of Chen et al. a multilayered fluidic system was used to sample effluent from both the basal and apical side of the tissue layer, elucidating the differences in growth factor expression under oxidative stress and highlighting a possible pathway or cause of disease development (150). The physical arrangement of microfluidic channels used in this system relied on sampling from one top channel and one bottom channel. Use of a fluidic channel array as the underlying network could allow sampling from discrete zones across the entire culture region. Each channel in the network could then be used to acquire sample from specific zones or ‘pixels’ just above the membrane that separates the sampling network from the microfluidic habitat above.

This idea was further developed with the demonstration of a microfluidic sampling device, a “chemistrode”, for routing fluid droplets to and from a flat substrate or surface (161). The entrained droplets capture temporal events and could be routed and analyzed off-line by any number of analytical techniques. By parking this chemistrode in a single location, dynamic chemical signaling events could be captured within a train of droplets. By scanning or rastering the chemistrode, or device of similar composition across a stable tissue or biofilm sample, it was shown that it was possible to map the chemical composition of a planar sample. Although physical disruption of the sample and lack a temporal resolution when rastering are potential drawbacks to such a system, this work points towards the promise of combining digital microfluidics with local sampling for next generation non-destructive chemical imaging.

4.3 Nanostructured Elements for Enhanced Label-less Analysis

Beyond using microfluidics to route chemical information off chip for analysis in conventional spectrometry and spectroscopy tools, the integration of nanoscale elements directly within or onto multi-scale fluidic platforms can be used to provide enhanced sensitivity and reduce the need for off-chip sample preparation. Once chemical information is routed away from the biological system of interest, conventional analytical tools, including those that rely on destruction of the sample, can be utilized without worry of perturbing the biological system of interest. Nanostructures capable of enhancing both MS and Raman signals derived from captured analytes can also provide an increased surface area for sample capture and re-collection under continuous flow. Established methods for fabricating and integrating nano- and microstructured collection elements within fluidic architectures have been described in the literature and have been used to realize Raman signal enhancements and enable quantitative analysis by mass spectrometry. For example, nanostructure geometries, primarily arrays of ‘posts’ of different

diameters, densities and aspect ratios have been created using a combination of electron beam lithography, anisotropic silicon etching and metal evaporation techniques (141, 162, 163). Aggregates of nanopatterned pillars, of varying randomly dispersed geometries, were created using electron beam lithography and reactive ion etching. Hot spots were identified via spectral mapping and could be replicated in precise patterns (164, 165). This points towards possibilities of integrating these enhancing patterns to create functional substrates. Other techniques have been developed to realize nanostructured surfaces that provide signal enhancements without the need for advanced lithographic tools. For example, SERS enhancements have been accomplished using pillar arrays created using a dewetting process (166). These nanoscale pillars can be produced across an entire substrate without the need for complex, time-consuming, or expensive lithographic processes. Enhancements as high as 10^7 were realized. Surface functionalization with silane reagents of varied composition (charge, hydrophobicity) can be carried out as necessary for targeted capture and sample clean-up. In contrast to these passive nanostructures, active nanoelectrode arrays (NEAs) and electrochemical zero-mode waveguides have been used to monitor and detect redox active species in space and time (167, 168).

5. OUTLOOK

The ideal of visualizing chemical environments within and around biological systems, while simultaneously monitoring their growth, development, and response to designed perturbations, offers tremendous opportunities to understand complex biological processes. Such capabilities will be essential for addressing the challenge of linking molecular events to phenotypic expression across system hierarchies. Nanoengineered materials and structures are bringing us closer to realizing this ideal. Advances in microscopy continue at a rapid pace,

offering researchers the ability to observe natural processes with unprecedented resolution over extended times. Nano-enabled tools are aiding these imaging advances and present practical and accessible approaches to observing biological systems at the molecular level. An assortment of nanomaterial structures is providing access to near field information and super resolution capabilities. Increased availability of these structures and simple means for increasing the field of view will be likely future directions. The intriguing possibility of using biomaterials as the optical components is also being considered (35, 169, 170).

While imaging technologies allow us to bear witness to physical and structural changes within such complex living systems, they often leave us in the dark as to the chemical cues and intermediate signaling mechanisms that are at work behind the scenes. Here, the ability to design and disperse nanoscale sensors that report on chemical environments is allowing us to see chemical changes occuring in living systems. This is an incredible feat as it provides the context for how local chemical differences drive structural and compositional changes of the biological system. Continued refinement of hybrid nanoparticle-based sensors that improve delivery and targeting to a wider range of biological systems is needed. Such advances will also benefit multiplexed chemical detection schemes so as to take advantage of the rich palette of fluorescence emission properties possible with nanomaterial labels.

Defining and controlling the physical and chemical environment is critical for evaluating biological systems. Microscale habitats with defined nanoscale features have unlocked new means for biological system studies at the molecular and cellular levels. Habitat designs that allow iterative control of the chemical environment and ordering of connections between these habitats will allow approximation of tissues and whole organisms. Further, the opportunity to use multiscale fluidic platforms to manipulate and sample the local environment will open the

door to understanding how living systems respond to local perturbations and adapt their function over time and space. Because the scales of these sampling techniques can be controlled, it is possible, in principal, to minimize unintentional disruption of the system of interest. Most significantly, local, minimally perturbing sampling will allow an interface to a larger suite of analytical measurement tools that are rarely considered for characterization of living systems.

Nanotechnologies that can be combined with functional habitats to allow enhanced optical imaging, local monitoring of environmental factors, and the extraction of chemical information such as those described above will be essential to facilitating the next generation of chemical imaging technologies. By themselves, these various nano-enabled technology thrusts provide a powerful arsenal for chemical imaging. In combination, a truly effective approach for linking the structural development of biological systems with spatial and temporal evolution of both system composition and the local chemical environment will be possible. The alignment of these nano-enabled imaging elements in varying ways have been described, and point towards the opportunities that fully integrated systems may provide. For example, hybrid core shell nanoparticles have been used for monitoring the acidification, in real-time, of a bacterial biofilm developing within a microfluidic environment under dynamically varied shear stress and nutrient concentrations (171). Optofluidic technologies, which combine microfluidic environments and integrated lens structures, including SILs have been developed and applied for imaging biological systems (172, 173). Further development and combination of nano-enabled chemical imaging tools are forthcoming. These advances will unlock new understandings of biological processes and are poised to unravel the chemical complexity of these systems.

ACKNOWLEDGEMENTS

Research supported by the U. S. Department of Energy (DOE), Office of Science, Office of Biological and Environmental Research, Genomic Science Program as part of the Plant Microbe Interfaces Scientific Focus Area (http://pmi.ornl.gov) and the Adaptive Biosystems Imaging project. Oak Ridge National Laboratory is managed by UT-Battelle, LLC, for the U.S. DOE under contract number DE-AC05-00OR22725. A portion of this research was conducted at the Center for Nanophase Materials Sciences, which is sponsored at Oak Ridge National Laboratory by the Scientific User Facilities Division, Office of Basic Energy Sciences, U.S. Department of Energy.

LITERATURE CITED

1. Thorn K. 2017. Genetically encoded fluorescent tags. *Molecular Biology of the Cell* 28: 848-57
2. Dunn WB, Ellis DI. 2005. Metabolomics: Current analytical platforms and methodologies. *TrAC Trends in Analytical Chemistry* 24: 285-94
3. Meyer E, Hug HJ, Bennewitz R. 2004. *Scanning Probe Microscopy: The Lab on a Tip*. Springer-Verlag Berlin Heidelberg
4. Lyra da Cunha MM, Trepout S, Messaoudi C, Wu T-D, Ortega R, et al. 2016. Overview of chemical imaging methods to address biological questions. *Micron* 84: 23-36
5. Watrous JD, Dorrestein PC. 2011. Imaging mass spectrometry in microbiology. *Nature Reviews Microbiology* 9: 683-94
6. Lanni EJ, Rubakhin SS, Sweedler JV. 2012. Mass spectrometry imaging and profiling of single cells. *Journal of proteomics* 75: 5036-51
7. Watrous JD, Dorrestein PC. 2011. Imaging mass spectrometry in microbiology. *Nature reviews. Microbiology* 9: 683-94
8. Allison DP, Mortensen NP, Sullivan CJ, Doktycz MJ. 2010. Atomic force microscopy of biological samples. *Wiley Interdisciplinary Reviews: Nanomedicine and Nanobiotechnology* 2: 618-34
9. Müller DJ, Dufrêne YF. 2011. Atomic force microscopy: a nanoscopic window on the cell surface. *Trends in Cell Biology* 21: 461-69
10. Sydor AM, Czymmek KJ, Puchner EM, Mennella V. 2015. Super-Resolution Microscopy: From Single Molecules to Supramolecular Assemblies. *Trends in Cell Biology* 25: 730-48

11. Lereu AL, Passian A, Dumas P. 2012. Near field optical microscopy: a brief review. *International Journal of Nanotechnology* 9: 488

12. Lewis A, Taha H, Strinkovski A, Manevitch A, Khatchatouriants A, et al. 2003. Near-field optics: from subwavelength illumination to nanometric shadowing. *Nat Biotechnol* 21: 1378-86

13. Richards D. 2003. Near-field microscopy: throwing light on the nanoworld. *Philosophical Transactions of the Royal Society of London Series a-Mathematical Physical and Engineering Sciences* 361: 2843-57

14. Mauser N, Hartschuh A. 2014. Tip-enhanced near-field optical microscopy. *Chem Soc Rev* 43: 1248-62

15. Schmid T, Opilik L, Blum C, Zenobi R. 2013. Nanoscale Chemical Imaging Using Tip-Enhanced Raman Spectroscopy: A Critical Review. *Angewandte Chemie International Edition* 52: 5940-54

16. Shalaev VM. 2008. Transforming light. *Science* 322: 384-86

17. Khorasaninejad M, Chen WT, Devlin RC, Oh J, Zhu AY, Capasso F. 2016. Metalenses at visible wavelengths: Diffraction-limited focusing and subwavelength resolution imaging. *Science* 352: 1190-94

18. Simovski CR, Belov PA, Atrashchenko AV, Kivshar YS. 2012. Wire metamaterials: physics and applications. *Adv Mater* 24: 4229-48

19. Valentine J, Zhang S, Zentgraf T, Ulin-Avila E, Genov DA, et al. 2008. Three-dimensional optical metamaterial with a negative refractive index. *Nature* 455: 376-79

20. Pendry JB. 2000. Negative Refraction Makes a Perfect Lens. *Physical Review Letters* 85: 3966-69

21. Liu Z, Lee H, Xiong Y, Sun C, Zhang X. 2007. Far-field optical hyperlens magnifying sub-diffraction-limited objects. *Science* 315: 1686

22. Smolyaninov II, Hung YJ, Davis CC. 2007. Magnifying superlens in the visible frequency range. *Science* 315: 1699-701

23. Ono A, Kato J, Kawata S. 2005. Subwavelength optical imaging through a metallic nanorod array. *Phys Rev Lett* 95: 267407

24. Kawata S, Ono A, Verma P. 2008. Subwavelength colour imaging with a metallic nanolens. *Nature Photonics* 2: 438-42

25. Casse BDF, Lu WT, Huang YJ, Gultepe E, Menon L, Sridhar S. 2010. Super-resolution imaging using a three-dimensional metamaterials nanolens. *Applied Physics Letters* 96: 023114

26. Mansfield SM, Kino GS. 1990. Solid immersion microscope. *Applied Physics Letters* 57: 2615-16

27. Lee JY, Hong BH, Kim WY, Min SK, Kim Y, et al. 2009. Near-field focusing and magnification through self-assembled nanoscale spherical lenses. *Nature* 460: 498-501

28. Fan W, Yan B, Wang ZB, Wu LM. 2016. Three-dimensional all-dielectric metamaterial solid immersion lens for subwavelength imaging at visible frequencies. *Science Advances* 2(8)

29. Kim MS, Scharf T, Haq MT, Nakagawa W, Herzig HP. 2011. Subwavelength-size solid immersion lens. *Optics Letters* 36: 3930-32

30. Jang J-W, Zheng Z, Lee O-S, Shim W, Zheng G, et al. 2010. Arrays of Nanoscale Lenses for Subwavelength Optical Lithography. *Nano Letters* 10: 4399-404

31. Kang D, Pang C, Kim SM, Cho HS, Um HS, et al. 2012. Shape-Controllable Microlens Arrays via Direct Transfer of Photocurable Polymer Droplets. *Advanced Materials* 24: 1709-15

32. Liau ZL, Liau AA, Porter JM, Salmon WC, Sheu SS, Chen JJ. 2015. Solid-immersion fluorescence microscopy with increased emission and super resolution. *Journal of Applied Physics* 117: 014502

33. Wang Z, Guo W, Li L, Luk'yanchuk B, Khan A, et al. 2011. Optical virtual imaging at 50 nm lateral resolution with a white-light nanoscope. *Nat Commun* 2: 218

34. Darafsheh A, Walsh GF, Dal Negro L, Astratov VN. 2012. Optical super-resolution by high-index liquid-immersed microspheres. *Applied Physics Letters* 101

35. Monks JN, Yan B, Hawkins N, Vollrath F, Wang Z. 2016. Spider Silk: Mother Nature's Bio-Superlens. *Nano Lett* 16: 5842-5

36. Darafsheh A, Wu GX, Yang S, Finlay JC. 2016. Super-resolution optical microscopy by using dielectric microwires. *Three-Dimensional and Multidimensional Microscopy: Image Acquisition and Processing Xxiii* Proceedings, SPIE Vol. 9713

37. Heifetz A, Kong SC, Sahakian AV, Taflove A, Backman V. 2009. Photonic Nanojets. *J Comput Theor Nanosci* 6: 1979-92

38. Allen KW, Farahi N, Li Y, Limberopoulos NI, Walker DE, et al. 2015. Super-resolution microscopy by movable thin-films with embedded microspheres: Resolution analysis. *Annalen der Physik* 527: 513-22

39. Li PY, Tsao Y, Liu YJ, Lou ZX, Lee WL, et al. 2016. Unusual imaging properties of superresolution microspheres. *Opt Express* 24: 16479-86

40. Yan YZ, Li L, Feng C, Guo W, Lee S, Hong MH. 2014. Microsphere-Coupled Scanning Laser Confocal Nanoscope for Sub-Diffraction-Limited Imaging at 25 nm Lateral Resolution in the Visible Spectrum. *Acs Nano* 8: 1809-16

41. Darafsheh A, Guardiola C, Palovcak A, Finlay JC, Carabe A. 2015. Optical super-resolution imaging by high-index microspheres embedded in elastomers. *Opt Lett* 40: 5-8

42. Du B, Ye Y-H, Hou J, Guo M, Wang T. 2015. Sub-wavelength image stitching with removable microsphere-embedded thin film. *Applied Physics A* 122:15

43. Krivitsky LA, Wang JJ, Wang Z, Luk'yanchuk B. 2013. Locomotion of microspheres for super-resolution imaging. *Sci Rep* 3: 3501

44. Wang F, Liu L, Yu H, Wen Y, Yu P, et al. 2016. Scanning superlens microscopy for non-invasive large field-of-view visible light nanoscale imaging. *Nat Commun* 7: 13748

45. Wang S, Zhang D, Zhang H, Han X, Xu R. 2015. Super-resolution optical microscopy based on scannable cantilever-combined microsphere. *Microsc Res Tech* 78: 1128-32

46. Li J, Liu W, Li T, Rozen I, Zhao J, et al. 2016. Swimming Microrobot Optical Nanoscopy. *Nano Lett* 16: 6604-09

47. Miklyaev YV, Asselborn SA, Zaytsev KA, Darscht MY. 2014. Superresolution microscopy in far-field by near-field optical random mapping nanoscopy. *Applied Physics Letters* 105: 113103

48. Li L, Guo W, Yan Y, Lee S, Wang T. 2013. Label-free super-resolution imaging of adenoviruses by submerged microsphere optical nanoscopy. *Light: Science & Applications* 2:e104

49. Yang H, Moullan N, Auwerx J, Gijs MAM. 2014. Super-Resolution Biological Microscopy Using Virtual Imaging by a Microsphere Nanoscope. *Small* 10: 1712-18

50. Rogers ET, Lindberg J, Roy T, Savo S, Chad JE, et al. 2012. A super-oscillatory lens optical microscope for subwavelength imaging. *Nat Mater* 11: 432-5

51. Wong AM, Eleftheriades GV. 2013. An optical super-microscope for far-field, real-time imaging beyond the diffraction limit. *Sci Rep* 3: 1715

52. Qin F, Huang K, Wu J, Teng J, Qiu CW, Hong M. 2017. A Supercritical Lens Optical Label-Free Microscopy: Sub-Diffraction Resolution and Ultra-Long Working Distance. *Adv Mater* 29 (8)

53. Brus LE. 1984. Electron‐electron and electron ‐ hole interactions in small semiconductor crystallites: The size dependence of the lowest excited electronic state. *The Journal of Chemical Physics* 80: 4403-09

54. Åkerman ME, Chan WCW, Laakkonen P, Bhatia SN, Ruoslahti E. 2002. Nanocrystal targeting in vivo. *Proceedings of the National Academy of Sciences* 99: 12617-21

55. Dubertret B, Skourides P, Norris DJ, Noireaux V, Brivanlou AH, Libchaber A. 2002. In Vivo Imaging of Quantum Dots Encapsulated in Phospholipid Micelles. *Science* 298: 1759-62

56. Jaiswal JK, Mattoussi H, Mauro JM, Simon SM. 2003. Long-term multiple color imaging of live cells using quantum dot bioconjugates. *Nat Biotech* 21: 47-51

57. Wu X, Liu H, Liu J, Haley KN, Treadway JA, et al. 2003. Immunofluorescent labeling of cancer marker Her2 and other cellular targets with semiconductor quantum dots. *Nat Biotech* 21: 41-46

58. De M, Ghosh PS, Rotello VM. 2008. Applications of Nanoparticles in Biology. *Advanced Materials* 20: 4225-41

59. Wang EC, Wang AZ. 2014. Nanoparticles and their applications in cell and molecular biology. *Integrative Biology* 6: 9-26

60. Sun Y-P, Zhou B, Lin Y, Wang W, Fernando KAS, et al. 2006. Quantum-Sized Carbon Dots for Bright and Colorful Photoluminescence. *Journal of the American Chemical Society* 128: 7756-57

61. Yang S-T, Cao L, Luo PG, Lu F, Wang X, et al. 2009. Carbon Dots for Optical Imaging in vivo. *Journal of the American Chemical Society* 131: 11308-09

62. Wang W, Nallathamby PD, Foster CM, Morrell-Falvey JL, Mortensen NP, et al. 2013. Volume labeling with Alexa Fluor dyes and surface functionalization of highly sensitive fluorescent silica (SiO2) nanoparticles. *Nanoscale* 5: 10369-75

63. Nallathamby PD, Mortensen NP, Palko HA, Malfatti M, Smith C, et al. 2015. New surface radiolabeling schemes of super paramagnetic iron oxide nanoparticles (SPIONs) for biodistribution studies. *Nanoscale* 7: 6545-55

64. Mortensen NP, Hurst GB, Wang W, Foster CM, Nallathamby PD, Retterer ST. 2013. Dynamic development of the protein corona on silica nanoparticles: composition and role in toxicity. *Nanoscale* 5: 6372-80

65. Zhang Y, Guo S, Cheng S, Ji X, He Z. 2017. Label-free silicon nanodots featured ratiometric fluorescent aptasensor for lysosomal imaging and pH measurement. *Biosensors and Bioelectronics* 94: 478-84

66. Wang L, Hu C, Shao L. 2017. The antimicrobial activity of nanoparticles: present situation and prospects for the future. *International Journal of Nanomedicine* 12: 1227-49

67. Sanvicens N, Pastells C, Pascual N, Marco MP. 2009. Nanoparticle-based biosensors for detection of pathogenic bacteria. *TrAC Trends in Analytical Chemistry* 28: 1243-52

68. Kloepfer J, Mielke R, Nadeau J. 2005. Uptake of CdSe and CdSe/ZnS quantum dots into bacteria via purine-dependent mechanisms. *Applied and environmental microbiology* 71: 2548-57

69. Baena JR, Lendl B. 2004. Raman spectroscopy in chemical bioanalysis. *Current Opinion in Chemical Biology* 8: 534-39

70. Abalde-Cela S, Carregal-Romero S, Coelho JP, Guerrero-Martínez A. 2016. Recent progress on colloidal metal nanoparticles as signal enhancers in nanosensing. *Advances in Colloid and Interface Science* 233: 255-70

71. Liu L, Jin M, Shi Y, Lin J, Zhang Y, et al. 2015. Optical integrated chips with micro and nanostructures for refractive index and SERS-based optical label-free sensing. In *Nanophotonics*, pp. 419

72. Opilik L, Schmid T, Zenobi R. 2013. Modern Raman Imaging: Vibrational Spectroscopy on the Micrometer and Nanometer Scales. *Annual Review of Analytical Chemistry* 6: 379-98

73. Zhou H, Yang D, Ivleva NP, Mircescu NE, Niessner R, Haisch C. 2014. SERS Detection of Bacteria in Water by in Situ Coating with Ag Nanoparticles. *Analytical Chemistry* 86: 1525-33

74. Polisetti S, Baig NF, Morales-Soto N, Shrout JD, Bohn PW. 2017. Spatial Mapping of Pyocyanin in *Pseudomonas aeruginosa* Bacterial Communities Using Surface Enhanced Raman Scattering. *Applied Spectroscopy* 71: 215-23

75. Polisetti S, Bible AN, Morrell-Falvey JL, Bohn PW. 2016. Raman chemical imaging of the rhizosphere bacterium *Pantoea* sp. YR343 and its co-culture with *Arabidopsis thaliana*. *Analyst* 141: 2175-82

76. Li JF, Huang YF, Ding Y, Yang ZL, Li SB, et al. 2010. Shell-isolated nanoparticle-enhanced Raman spectroscopy. *Nature* 464: 392-95

77. Li J-F, Zhang Y-J, Ding S-Y, Panneerselvam R, Tian Z-Q. 2017. Core–Shell Nanoparticle-Enhanced Raman Spectroscopy. *Chemical Reviews* 117: 5002-69

78. Zhu A, Qu Q, Shao X, Kong B, Tian Y. 2012. Carbon-Dot-Based Dual-Emission Nanohybrid Produces a Ratiometric Fluorescent Sensor for In Vivo Imaging of Cellular Copper Ions. *Angewandte Chemie* 124: 7297-301

79. Yang R, Guo X, Jia L, Zhang Y. 2017. A fluorescent "on-off-on" assay for selective recognition of Cu(II) and glutathione based on modified carbon nanodots, and its application to cellular imaging. *Microchimica Acta* 184: 1143-50

80. Wang H, Zhang P, Chen J, Li Y, Yu M, et al. 2017. Polymer nanoparticle-based ratiometric fluorescent probe for imaging Hg2+ ions in living cells. *Sensors and Actuators B: Chemical* 242: 818-24

81. Yan F, Kong D, Luo Y, Ye Q, He J, et al. 2016. Carbon dots serve as an effective probe for the quantitative determination and for intracellular imaging of mercury(II). *Microchimica Acta* 183: 1611-18

82. Hidalgo G, Burns A, Herz E, Hay AG, Houston PL, et al. 2009. Functional Tomographic Fluorescence Imaging of pH Microenvironments in Microbial Biofilms by Use of Silica Nanoparticle Sensors. *Applied and Environmental Microbiology* 75: 7426-35

83. Chen J, Tang Y, Wang H, Zhang P, Li Y, Jiang J. 2016. Design and fabrication of fluorescence resonance energy transfer-mediated fluorescent polymer nanoparticles for ratiometric sensing of lysosomal pH. *Journal of Colloid and Interface Science* 484: 298-307

84. Jiang Y, Wang M, Hardie J, Tonga GY, Ray M, et al. 2016. Chemically Engineered Nanoparticle-Protein Interface for Real-Time Cellular Oxidative Stress Monitoring. *Small* 12: 3775-79

85. Vaishanav SK, Korram J, Nagwanshi R, Ghosh KK, Satnami ML. 2017. Mn2+ doped-CdTe/ZnS modified fluorescence nanosensor for detection of glucose. *Sensors and Actuators B: Chemical* 245: 196-204

86. Huang S, Wang L, Huang C, Su W, Xiao Q. 2017. Label-free and ratiometric fluorescent nanosensor based on amino-functionalized graphene quantum dots coupling catalytic G-quadruplex/hemin DNAzyme for ultrasensitive recognition of human telomere DNA. *Sensors and Actuators B: Chemical* 245: 648-55

87. Liang S-S, Qi L, Zhang R-L, Jin M, Zhang Z-Q. 2017. Ratiometric fluorescence biosensor based on CdTe quantum and carbon dots for double strand DNA detection. *Sensors and Actuators B: Chemical* 244: 585-90

88. Qian J, Wang K, Wang C, Ren C, Liu Q, et al. 2017. Ratiometric fluorescence nanosensor for selective and visual detection of cadmium ions using quencher displacement-induced fluorescence recovery of CdTe quantum dots-based hybrid probe. *Sensors and Actuators B: Chemical* 241: 1153-60

89. Fu H, Ji Z, Chen X, Cheng A, Liu S, et al. 2017. A versatile ratiometric nanosensing approach for sensitive and accurate detection of Hg2+ and biological thiols based on new fluorescent carbon quantum dots. *Analytical and Bioanalytical Chemistry* 409: 2373-82

90. Xu H, Zhang K, Liu Q, Liu Y, Xie M. 2017. Visual and fluorescent detection of mercury ions by using a dually emissive ratiometric nanohybrid containing carbon dots and CdTe quantum dots. *Microchimica Acta* 184: 1199-206

91. Donmez M, Yilmaz MD, Kilbas B. 2017. Fluorescent detection of dipicolinic acid as a biomarker of bacterial spores using lanthanide-chelated gold nanoparticles. *Journal of Hazardous Materials* 324, Part B: 593-98

92. Xiang G-Q, Ren Y, Xia Y, Mao W, Fan C, et al. 2017. Carbon-dot-based dual-emission silica nanoparticles as a ratiometric fluorescent probe for Bisphenol A. *Spectrochimica Acta Part A: Molecular and Biomolecular Spectroscopy* 177: 153-57

93. Campos BB, Contreras-Cáceres R, Bandosz TJ, Jiménez-Jiménez J, Rodríguez-Castellón E, et al. 2017. Carbon dots coated with vitamin B12 as selective ratiometric nanosensor for phenolic carbofuran. *Sensors and Actuators B: Chemical* 239: 553-61

94. Lu H, Koo LY, Wang WM, Lauffenburger DA, Griffith LG, Jensen KF. 2004. Microfluidic Shear Devices for Quantitative Analysis of Cell Adhesion. *Anal Chem* 76: 5257-64

95. Takayama S, Ostuni E, LeDuc P, Naruse K, Ingber DE. 2001. Laminar flows: subcellular positioning of small molecules. *Nature* 411: 1016

96. Takayama S, Ostuni E, LeDuc P, Naruse K, Ingber DE, Whitesides GM. 2003. Selective Chemical Treatment of Cellular Microdomains Using Multiple Laminar Streams. *Chemistry \& biology* 10: 123-30

97. Lucchetta EM, Munson MS, Ismagilov RF. 2006. Characterization of the local temperature in space and time around a developing Drosophila embryo in a microfluidic device. *Lab on a Chip* 6: 185-90

98. Qin D, Xia Y, Whitesides GM. 1997. Elastomeric Light Valves. *Advanced Materials* 9: 407-10

99. Duffy DC, McDonald JC, Schueller OJ, Whitesides GM. 1998. Rapid Prototyping of Microfluidic Systems in Poly(dimethylsiloxane). *Anal Chem* 70: 4974-84

100. McDonald JC, Duffy DC, Anderson JR, Chiu DT, Wu H, et al. 2000. Fabrication of microfluidic systems in poly(dimethylsiloxane). *Electrophoresis* 2: 27-40

101. Thorsen T, Maerkl SJ, Quake SR. 2002. Microfluidic large-scale integration. *Science* 298: 580-4

102. Khademhosseini A, Yeh J, Eng G, Karp J, Kaji H, et al. 2005. Cell docking inside microwells within reversibly sealed microfluidic channels for fabricating multiphenotype cell arrays. *Lab Chip* 5: 1380-6

103. Toh YC, Zhang C, Zhang J, Khong YM, Chang S, et al. 2007. A novel 3D mammalian cell perfusion-culture system in microfluidic channels. *Lab Chip* 7: 302-9

104. Tourovskaia A, Figueroa-Masot X, Folch A. 2005. Differentiation-on-a-chip: A microfluidic platform for long-term cell culture studies. *Lab on a Chip* 5: 14-19

105. Meyvantsson I, Beebe DJ. 2008. Cell Culture Models in Microfluidic Systems. *Annual Review of Analytical Chemistry* 1: 423-49

106. Abaci HE, Shuler ML. 2015. Human-on-a-chip design strategies and principles for physiologically based pharmacokinetics/pharmacodynamics modeling. *Integrative Biology* 7: 383-91

107. Huh D, Matthews BD, Mammato A, Montoya-Zavala M, Hsin HY, Ingber DE. 2010. Reconstituting Organ-Level Lung Functions on a Chip. *Science* 328: 1662-8

108. Mahler GJ, Esch MB, Glahn RP, Shuler ML. 2009. Characterization of a gastrointestinal tract microscale cell culture analog used to predict drug toxicity. *Biotechnol Bioeng* 104: 193-205

109. Powers MJ, Domansky K, Kaazempur Mofrad MR, Kalezi A, Capitano A, et al. 2002. A microfabricated array bioreactor for perfused 3D liver culture. *Biotechnology and Bioengineering* 78: 257-69

110. Grossmann G, Guo WJ, Ehrhardt DW, Frommer WB, Sit RV, et al. 2011. The RootChip: an integrated microfluidic chip for plant science. *Plant Cell* 23: 4234-40

111. Grossmann G, Meier M, Cartwright HN, Sosso D, Quake SR, et al. 2012. Time-lapse Fluorescence Imaging of Arabidopsis Root Growth with Rapid Manipulation of The Root Environment Using The RootChip. *Journal of Visualized Experiments : JoVE*

112. Jiang H, Xu Z, Aluru MR, Dong L. 2014. Plant chip for high-throughput phenotyping of Arabidopsis. *Lab on a Chip* 14: 1281-93

113. Meier M, Lucchetta EM, Ismagilov RF. 2010. Chemical stimulation of the *Arabidopsis thaliana* root using multi-laminar flow on a microfluidic chip. *Lab on a Chip* 10: 2147

114. Deng J, Orner EP, Chau JF, Anderson EM, Kadilak AL, et al. 2015. Synergistic effects of soil microstructure and bacterial EPS on drying rate in emulated soil micromodels. *Soil Biology and Biochemistry* 83: 116-24

115. Rubinstein RL, Kadilak AL, Cousens VC, Gage DJ, Shor LM. 2015. Protist-facilitated particle transport using emulated soil micromodels. *Environ Sci Technol* 49: 1384-91

116. Stanley CE, Grossmann G, i Solvas XC, deMello AJ. 2016. Soil-on-a-Chip: microfluidic platforms for environmental organismal studies. *Lab Chip* 16: 228-41

117. Massalha H, Korenblum E, Malitsky S, Shapiro OH, Aharoni A. 2017. Live imaging of root-bacteria interactions in a microfluidics setup. *Proceedings of the National Academy of Sciences of the United States of America* 114: 4549-54

118. Parashar A, Pandey S. 2011. Plant-in-chip: Microfluidic system for studying root growth and pathogenic interactions in Arabidopsis. *Applied Physics Letters* 98: 263703

119. Craighead HG, Turner SW, Davis RC, James C, Kam L, et al. 1998. Chemical and Topographical Surface Modification for Control of Central Nervous System Cell Adhesion. *Journal of Biomedical Microdevices* 1: 49-64

120. James CD, Davis RC, Kam L, Craighead HG, Isaacson M, et al. 1998. Patterned Protein Layers on Solid Substrates by Thin Stamp Microcontact Printing. *Langmuir* 14: 741-44

121. Geng T, Bredeweg EL, Szymanski CJ, Liu B, Baker SE, et al. 2015. Compartmentalized microchannel array for high-throughput analysis of single cell polarized growth and dynamics. *Scientific Reports* 5: 16111

122. Chen CS, Mrksich M, Huang S, Whitesides GM, Ingber DE. 1997. Geometric control of cell life and death. *Science* 276: 1425-8

123. Vargis E, Peterson CB, Morrell-Falvey JL, Retterer ST, Collier CP. 2014. The effect of retinal pigment epithelial cell patch size on growth factor expression. *Biomaterials* 35: 3999-4004

124. Hansen RR, Hinestrosa JP, Shubert KR, Morrell-Falvey JL, Pelletier DA, et al. 2013. Lectin-Functionalized Poly(glycidyl methacrylate)- block-poly(vinyldimethyl azlactone) Surface Scaffolds for High Avidity Microbial Capture. *Biomacromolecules* 14: 3742-48

125. Hansen R, Shubert K, Morrell-Falvey J, Lokitz B, Doktycz M, Retterer S. 2014. Microstructured Block Copolymer Surfaces for Control of Microbe Adhesion and Aggregation. *Biosensors* 4: 63-75

126. Bhatia S, Yarmush ML, Toner M. 1997. Controlling Cell Interactions by Micropatterning in Co-Cultures: Hepatocytes and 3T3 Fibroblasts. *Journal of Biomedical Materials Research* 34: 189-99

127. Timm CM, Hansen RR, Doktycz MJ, Retterer ST, Pelletier DA. 2015. Microstencils to generate defined, multi-species patterns of bacteria. *Biomicrofluidics* 9: 064103

128. Keymer JE, Galajda P, Muldoon C, Park S, Austin RH. 2006. Bacterial metapopulations in nanofabricated landscapes. *Proceedings of the National Academy of Sciences* 103: 17290-95

129. Keymer JE, Galajda P, Lambert G, Liao D, Austin RH. 2008. Computation of mutual fitness by competing bacteria. *Proceedings of the National Academy of Sciences of the United States of America* 105: 20269-73

130. Shankles PG, Timm AC, Doktycz MJ, Retterer ST. 2015. Fabrication of nanoporous membranes for tuning microbial interactions and biochemical reactions. *Journal of Vacuum Science \& Technology B, Nanotechnology and Microelectronics: Materials, Processing, Measurement, and Phenomena* 33: 06FM03

131. Beebe DJ, Moore JS, Bauer JM, Yu Q, Liu RH, et al. 2000. Functional hydrogel structures for autonomous flow control inside microfluidic channels. *Nature* 404: 588-90

132. Connell JL, Kim J, Shear JB, Bard AJ, Whiteley M. 2014. Real-time monitoring of quorum sensing in 3D-printed bacterial aggregates using scanning electrochemical microscopy. *Proceedings of the National Academy of Sciences* 111: 18255-60

133. Connell JL, Ritschdorff ET, Whiteley M, Shear JB. 2013. 3D printing of microscopic bacterial communities. *Proceedings of the National Academy of Sciences of the United States of America* 110: 18380-85

134. Dertinger SKW, Chiu DT, Jeon NL, Whitesides GM. 2001. Generation of Gradients Having Complex Shapes Using Microfluidic Networks. *Anal Chem* 73: 1240-46

135. Mao H, Cremer PS, Manson MD. 2003. A sensitive, versatile microfluidic assay for bacterial chemotaxis. *Proc Natl Acad Sci U S A* 100: 5449-54

136. Ahmed T, Stocker R. 2008. Experimental Verification of the Behavioral Foundation of Bacterial Transport Parameters Using Microfluidics. *Biophysical Journal* 95: 4481-93

137. Kovarik ML, Brown PJB, Kysela DT, Berne C, Kinsella AC, et al. 2010. Microchannel-Nanopore Device for Bacterial Chemotaxis Assays. *Analytical Chemistry* 82: 9357-64

138. Stocker R, Seymour JR, Samadani A, Hunt DE, Polz MF. 2008. Rapid chemotactic response enables marine bacteria to exploit ephemeral microscale nutrient patches. *PNAS* 105: 4209-14

139. Abhyankar VV, Lokuta MA, Huttenlocher A, Beebe DJ. 2006. Characterization of a membrane-based gradient generator for use in cell-signaling studies. *Lab on a Chip* 6: 389-93

140. Abhyankar VV, Toepke MW, Cortesio CL, Lokuta MA, Huttenlocher A, Beebe DJ. 2008. A platform for assessing chemotactic migration within a spatiotemporally defined 3D microenvironment. *Lab on a Chip* 8: 1507-15

141. Walker GM, Sai J, Richmond A, Stremler M, Chung CY, Wikswo JP. 2005. Effects of flow and diffusion on chemotaxis studies in a microfabricated gradient generator. *Lab on a Chip* 5: 611-18

142. Branchford BR, Ng CJ, Neeves KB, Di Paola J. 2015. Microfluidic technology as an emerging clinical tool to evaluate thrombosis and hemostasis. *Thrombosis research* 136: 13-19

143. Neeves KB, Diamond SL. 2008. A membrane-based microfluidic device for controlling the flux of platelet agonists into flowing blood. *Lab on a Chip* 8: 701-09

144. Neeves KB, McCarty OJ, Reininger AJ, Sugimoto M, King MR, Biorheology Subcommittee of the SSCotI. 2014. Flow-dependent thrombin and fibrin generation in vitro: opportunities for standardization: communication from SSC of the ISTH. *J Thromb Haemost* 12: 418-20

145. Schoeman RM, Rana K, Danes N, Lehmann M, Di Paola JA, et al. 2017. A Microfluidic Model of Hemostasis Sensitive to Platelet Function and Coagulation. *Cellular and Molecular Bioengineering* 10: 3-15

146. Biswas I, Ghosh R, Sadrzadeh M, Kumar A. 2016. Nonlinear deformation and localized failure of bacterial streamers in creeping flows. *Sci Rep* 6: 32204

147. Hassanpourfard M, Ghosh R, Thundat T, Kumar A. 2016. Dynamics of bacterial streamers induced clogging in microfluidic devices. *Lab Chip* 16: 4091-96

148. Marty A, Causserand C, Roques C, Bacchin P. 2014. Impact of tortuous flow on bacteria streamer development in microfluidic system during filtration. *Biomicrofluidics* 8: 014105

149. Yazdi S, Ardekani AM. 2012. Bacterial aggregation and biofilm formation in a vortical flow. *Biomicrofluidics* 6: 44114

150. Chen LJ, Ito S, Kai H, Nagamine K, Nagai N, et al. 2017. Microfluidic co-cultures of retinal pigment epithelial cells and vascular endothelial cells to investigate choroidal angiogenesis. *Sci Rep* 7: 3538

151. Retterer ST, Siuti P, Choi CK, Thomas DK, Doktycz MJ. 2010. Development and fabrication of nanoporous silicon-based bioreactors within a microfluidic chip. *Lab Chip* 10: 1174-81

152. Siuti P, Retterer ST, Choi CK, Doktycz MJ. 2012. Enzyme reactions in nanoporous, picoliter volume containers. *Anal Chem* 84: 1092-7

153. Siuti P, Retterer ST, Doktycz MJ. 2011. Continuous protein production in nanoporous, picolitre volume containers. *Lab on a Chip* 11: 3523-29

154. Timm AC, Shankles PG, Foster CM, Doktycz MJ, Retterer ST. 2015. Characterization of extended channel bioreactors for continuous-flow protein production. *Journal of Vacuum Science \& Technology B* 33: 06FM02

155. Timm AC, Shankles PG, Foster CM, Doktycz MJ, Retterer ST. 2016. Toward Microfluidic Reactors for Cell-Free Protein Synthesis at the Point-of-Care. *Small* 12: 810-17

156. Hung PJ, Lee PJ, Sabounchi P, Lin R, Lee LP. 2005. Continuous perfusion microfluidic cell culture array for high-throughput cell-based assays. *Biotechnology and Bioengineering* 89: 1-8

157. Flachsbart BR, Wong K, Iannacone JM, Abante EN, Vlach RL, et al. 2006. Design and fabrication of a multilayered polymer microfluidic chip with nanofluidic interconnects via adhesive contact printing. *Lab on a Chip* 6: 667-8

158. Gatimu EN, King TL, Sweedler JV, Bohn PW. 2007. Three-dimensional integrated microfluidic architectures enabled through electrically switchable nanocapillary array membranes. *Biomicrofluidics* 1: 21502

159. Li F, Guijt RM, Breadmore MC. 2016. Nanoporous Membranes for Microfluidic Concentration Prior to Electrophoretic Separation of Proteins in Urine. *Anal Chem* 88: 8257-63

160. Tan W, Desai TA. 2005. Microscale multilayer cocultures for biomimetic blood vessels. *J Biomed Mater Res A* 72: 146-60

161. Chen D, Du W, Liu Y, Liu W, Kuznetsov A, et al. 2008. The chemistrode: A droplet-based microfluidic device for stimulation and recording with high temporal, spatial, and chemical resolution. *Proceedings of the National Academy of Sciences* 105: 16843-48

162. Walker BN, Antonakos C, Retterer ST, Vertes A. 2013. Metabolic Differences in Microbial Cell Populations Revealed by Nanophotonic Ionization. *Angewandte Chemie International Edition* 52: 3650--53

163. Walker BN, Stolee JA, Pickel DL, Retterer ST, Vertes A. 2010. Assessment of laser-induced thermal load on silicon nanostructures based on ion desorption yields. *Applied Physics A* 101: 539-44

164. Polemi A, Wells SM, Lavrik NV, Sepaniak MJ, Shuford KL. 2010. Local Field Enhancement of Pillar Nanosurfaces for SERS. *The Journal of Physical Chemistry C* 114: 18096--102

165. Wells SM, Retterer SD, Oran JM, Sepaniak MJ. 2009. Controllable Nanofabrication of Aggregate-like Nanoparticle Substrates and Evaluation for Surface-Enhanced Raman Spectroscopy. *ACS Nano* 3: 3845--53

166. Agapov RL, Srijanto B, Fowler C, Briggs D, Lavrik NV, Sepaniak MJ. 2013. Lithography-free approach to highly efficient, scalable SERS substrates based on disordered clusters of disc-on-pillar structures. *Nanotechnology* 24: 505302

167. Fu K, Han D, Ma C, Bohn PW. 2017. Ion selective redox cycling in zero-dimensional nanopore electrode arrays at low ionic strength. *Nanoscale* 9: 5164-71

168. Han D, Crouch G, Fu K, Zaino Iii LP, Bohn PW. 2017. Single-molecule spectroelectrochemical cross-correlation during redox cycling in recessed dual ring electrode zero-mode waveguides. *Chemical Science* 8: 5345-55

169. De Tommasi E, De Luca AC, Lavanga L, Dardano P, De Stefano M, et al. 2014. Biologically enabled sub-diffractive focusing. *Opt Express* 22: 27214-27

170. Schuergers N, Lenn T, Kampmann R, Meissner MV, Esteves T, et al. 2016. Cyanobacteria use micro-optics to sense light direction. *Elife* 5

171. Gashti MP, Asselin J, Barbeau J, Boudreau D, Greener J. 2016. A microfluidic platform with pH imaging for chemical and hydrodynamic stimulation of intact oral biofilms. *Lab on a Chip* 16: 1412-19

172. Gambin Y, Legrand O, Quake SR. 2006. Microfabricated rubber microscope using soft solid immersion lenses. *Applied Physics Letters* 88: 174102

173. Psaltis D, Quake SR, Yang C. 2006. Developing optofluidic technology through the fusion of microfluidics and optics. *Nature* 442: 381-6

174. Lismont M, Páez CA, Dreesen L. 2015. A one-step short-time synthesis of Ag@SiO2 core–shell nanoparticles. *Journal of Colloid and Interface Science* 447: 40-49

175. Millet LJ, Doktycz MJ, Retterer ST. 2015. Nanofluidic interfaces in microfluidic networks. *Journal of Vacuum Science \& Technology B* 33: 06FM01

176. Walker BN, Stolee JA, Vertes A. 2012. Nanophotonic ionization for ultratrace and single-cell analysis by mass spectrometry. *Anal Chem* 84: 7756-62

177. Connell JL, Wessel AK, Parsek MR, Ellington AD, Whiteley M, Shear JB. 2010. Probing Prokaryotic Social Behaviors with Bacterial Lobster Traps. *mBio* 1: e00202--10--e02--17

178. Hatab NA, Hsueh C-H, Gaddis AL, Retterer ST, Li J-H, et al. 2010. Free-Standing Optical Gold Bowtie Nanoantenna with Variable Gap Size for Enhanced Raman Spectroscopy. *Nano Letters* 10: 4952--55

FIGURE CAPTIONS

Figure 1: Overview of approaches to nano-enabled chemical imaging. (middle) Microscale fluidic habitats for cellular system can define the chemical and physical environment. (top left) Nanoparticles can be employed for targeting and for acting as sentinels of chemical and environmental conditions. Shown are $AgSiO_2$ core-shell nanoparticles. Reprinted from (174), Copyright 2015, with permission from Elsevier. (bottom left) Various metamaterials and nanoscale optical tools, such as nanoscale solid immersion lenses can facilitate the resolution of features below the diffraction limit. Reprinted with permission from Macmillan Publishers Ltd: Nature (27), Copyright 2009. (bottom right) Membrane and nanoporous structures, such as a focused ion beam milled pore in a nanofluidic conduit, can be integrated with multiscale fluidic habitats for sampling chemical information. Reprinted with permission from (175). Copyright 2015, American Vacuum Society. (top right) The detection and enhancement of chemical signals can be facilitated by various nanostructure geometries such as silicon nanopost arrays. Reprinted with permission from (176), Copyright 2012, American Chemical Society.

Figure 2: Nano-enabled approaches to optical imaging allow high resolution. (a) Non-invasive white-light and fluorescence microscopy images of a C2C12 cell without and with the

enhancement of a 56 μm-diameter microsphere superlens and a 100× (numerical aperture=0.8) objective. Actin filaments, labelled by Alexa Fluor 488-phalloidin are clearly observed. Scale bars, 5 μm. Reprinted with permission from (44). (b) Super-resolution imaging at long working distances using a supercritical lens is described. At left is a schematic of SCL microscopy. At right are images of a nanoscale Big Dipper used to demonstrate the resolution enhancement. Compared images were collected by scanning electron microscopy (SEM), transmission mode microscopy (T-mode), laser scanning confocal microscopy (LSCM) and super critical lens microscopy (SCL). Reprinted with permission from (52) Copyright 2016, John Wiley and Sons.

Figure 3: Schematic diagram and biological application of ratiometric nanoparticles. (a) Schematic diagram of ratiometric nanoparticle showing a reference core particle surrounded by a shell particle sensitive to chemical or environmental signals. (b) An example of ratiometric nanoparticles used to detect pH in an *E. coli* biofilm. Reprinted with permission from (82), Copyright 2009, American Society for Microbiology.

Figure 4: Examples of integrated membrane structures. (a) A combination of electron beam lithography, photolithography and reactive ion etching can be used to create multiscale fluidic systems with fluidic channels and chambers separated by barriers of controlled porosity. (b, left) Replicate molding, and soft lithography can be used to create culture chambers in which mammalian or bacterial cultures (left brightfield, right fluorescence) can be maintained and imaged over extended periods of time. Porous barriers (inset) are used to keep different species physically separated while allowing efficient nutrient supply and chemical exchange between culture chambers. (b, right) Expression of green fluorescent protein (GFP) in response to a

signaling molecule being secreted by bacteria in the lower chamber is demonstrated. (a-b) Reprinted with permission from (130). Copyright 2015, American Vacuum Society. (c) A dynamic mask-based multiphoton lithography process was used to define traps for individual *P. aeruginosa* cells . A single trapped bacterium is shown growing into a picoliter colony. An SEM micrograph of a trap is shown (bottom). Scale bar is 5μm. Reprinted with permission from (177). (d) A commercial membrane sandwiched between two PDMS channels allowed for controlled flux of ADP into flowing blood. Platelet aggregation was monitored by confocal fluorescence imaging (not shown) and scanning electron microscopy. Scale bar 5μm. Reproduced from (143) with permission of The Royal Society of Chemistry.

Figure 5: Examples of nano structure enhancement elements. (a) SEM micrograph (30º tilt) of silicon nanopost arrays (NAPAs) with a height of 1000 nm and diameter of 100 nm, H/D = 10. Controlling the aspect ratio of these pillars is essential to optimizing ion yields during during laser desorption ionization (LDI) mass spectrometry. Reprinted with permission from (176), Copyright 2012, American Chemical Society. (B) SEM image of a free-standing gold bowtie nanoantennae with a gap of ~8 nm that was created using a combination of electron beam lithography, anisotropic silicon etching, and Au evaporation. Both gap size and elevation height contribute to enhancement in Raman signals as high as 10^{11} . Reprinted with permission from (178), Copyright 2010, American Chemical Society. .(c) A Schematic showing the operation and structure of an electrochemical zero mode waveguide. These devices allow direct correlation of optical and electrochemical signals during single electron exchange events within the zeptoliter waveguide volume. (d) An SEM micrograph showing the E-ZMW structure. (c-d) Reprinted with permission from (168).

Figure 1.

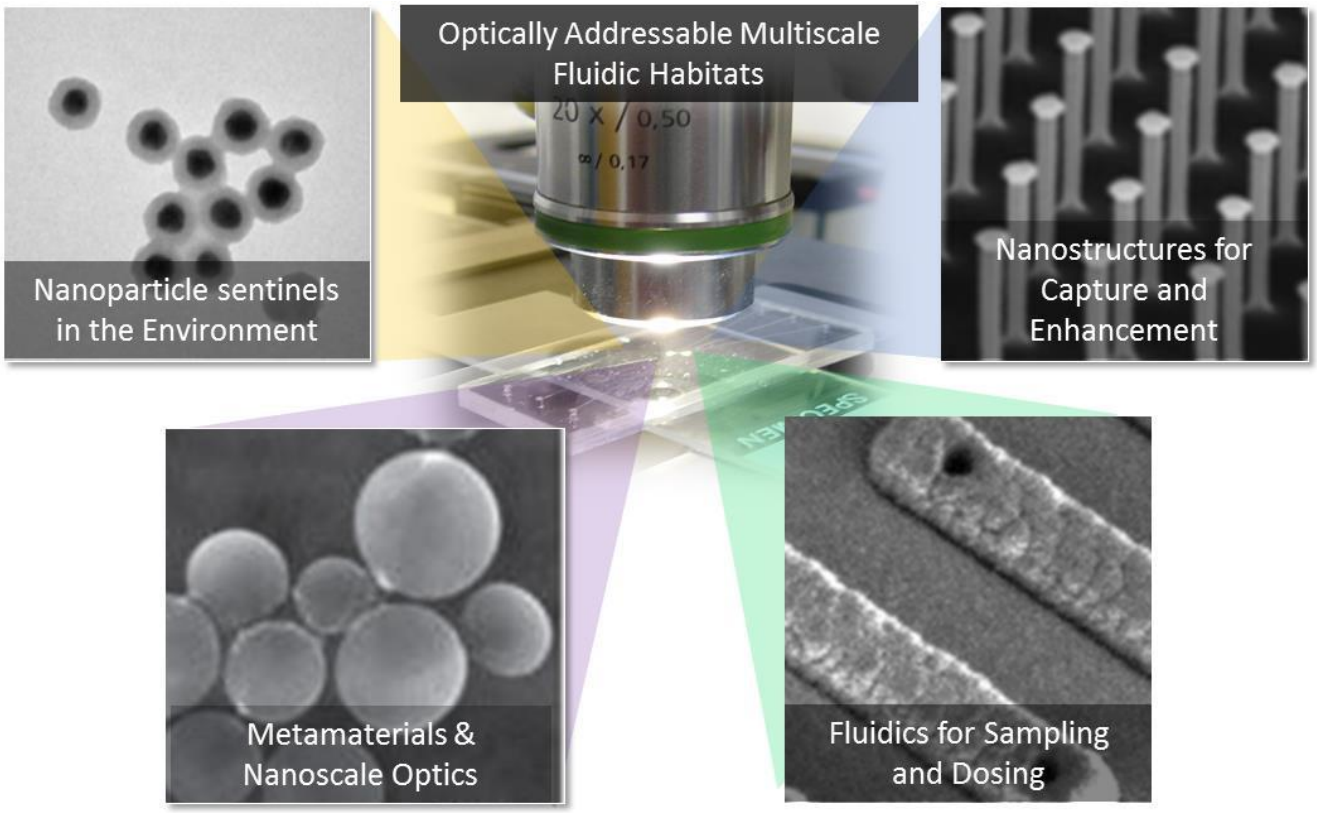
Optically Addressable Multiscale Fluidic Habitats
Nanoparticle sentinels in the Environment
Nanostructures for Capture and Enhancement
Metamaterials & Nanoscale Optics
Fluidics for Sampling and Dosing

Figure 2.

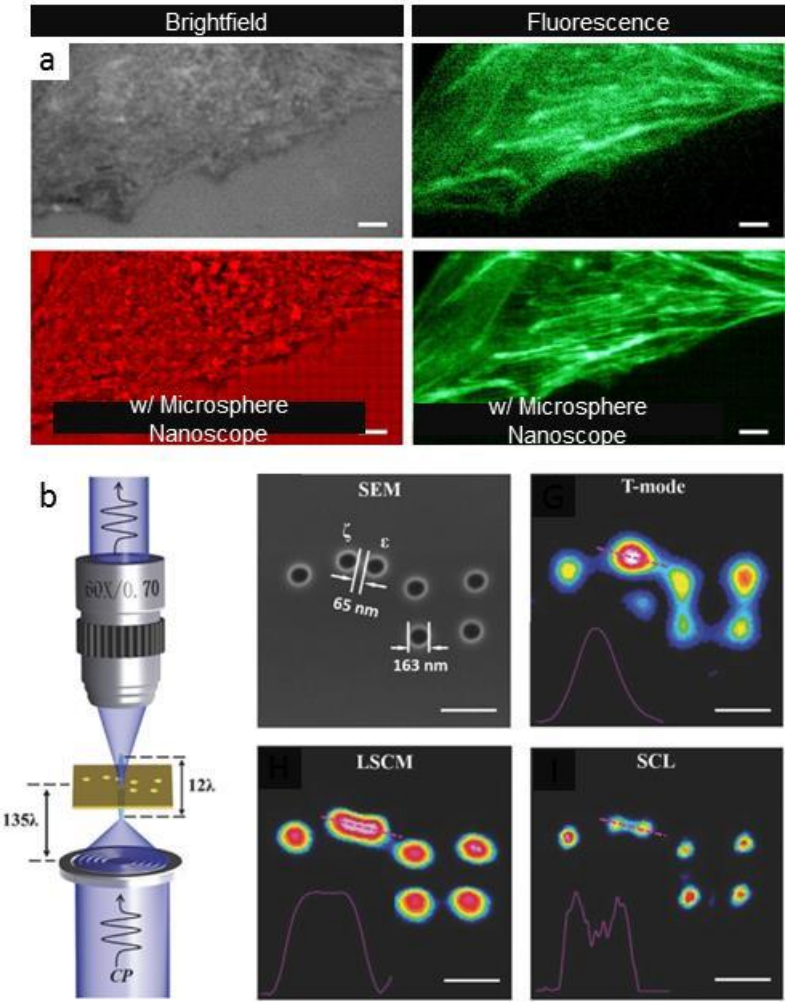
Brightfield
Fluorescence
a
w/ Microsphere Nanoscope
w/ Microsphere Nanoscope
b
60X/0.70
CP
SEM
65 nm
163 nm
T-mode
LSCM
SCL

Figure 3.

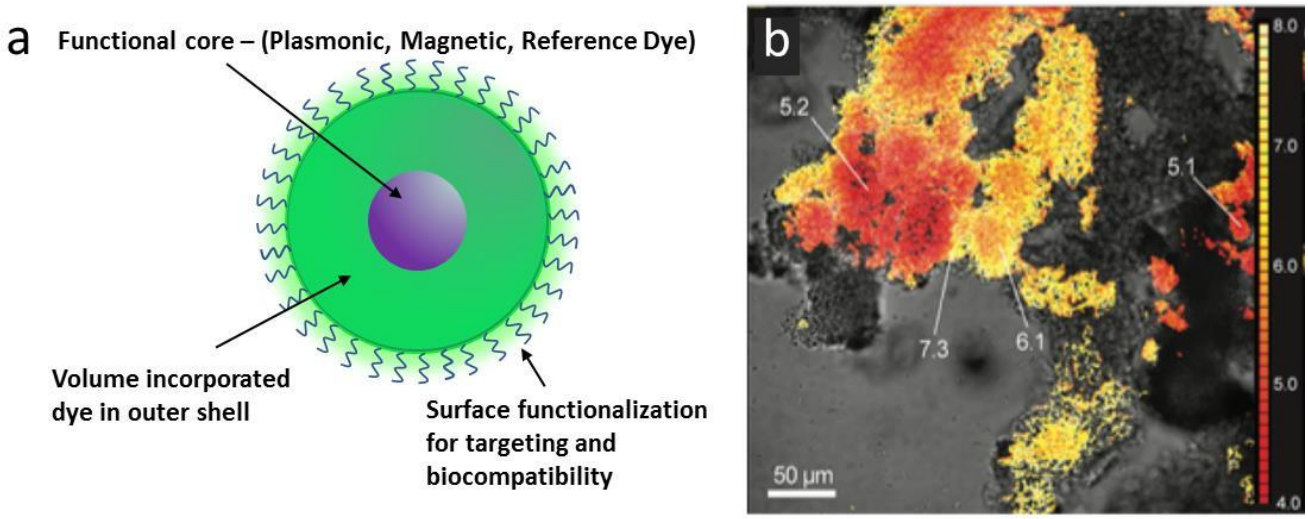
a
Functional core – (Plasmonic, Magnetic, Reference Dye)
Volume incorporated dye in outer shell
Surface functionalization for targeting and biocompatibility
b
5.2
5.1
7.3
6.1
50 µm
8.0
7.0
6.0
5.0
4.0

Figure 4.

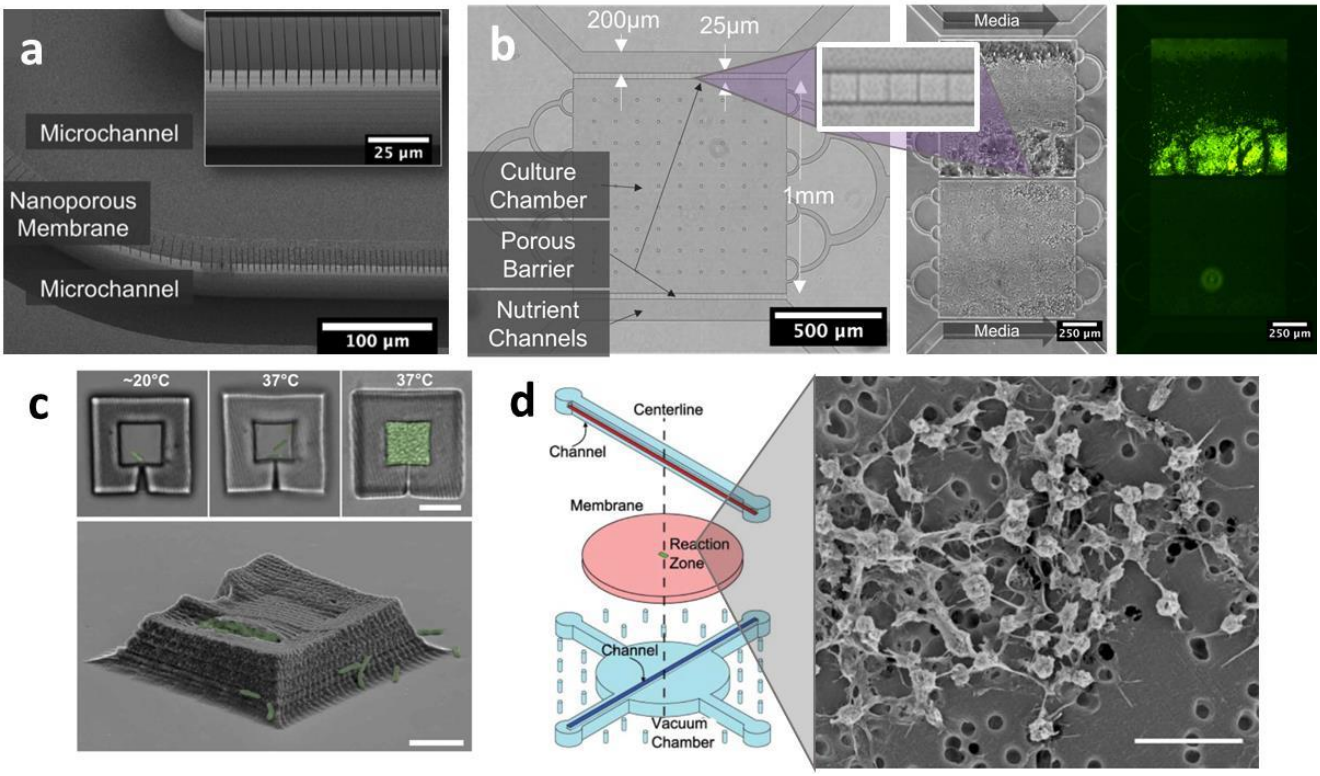
a
Microchannel
25 µm
Nanoporous Membrane
Microchannel
100 µm
b
200µm
25µm
Culture Chamber
Porous Barrier
Nutrient Channels
1mm
500 µm
Media
Media
250 µm
250 µm
c
~20°C
37°C
37°C
d
Centerline
Channel
Membrane
Reaction Zone
Channel
Vacuum Chamber

Figure 5.

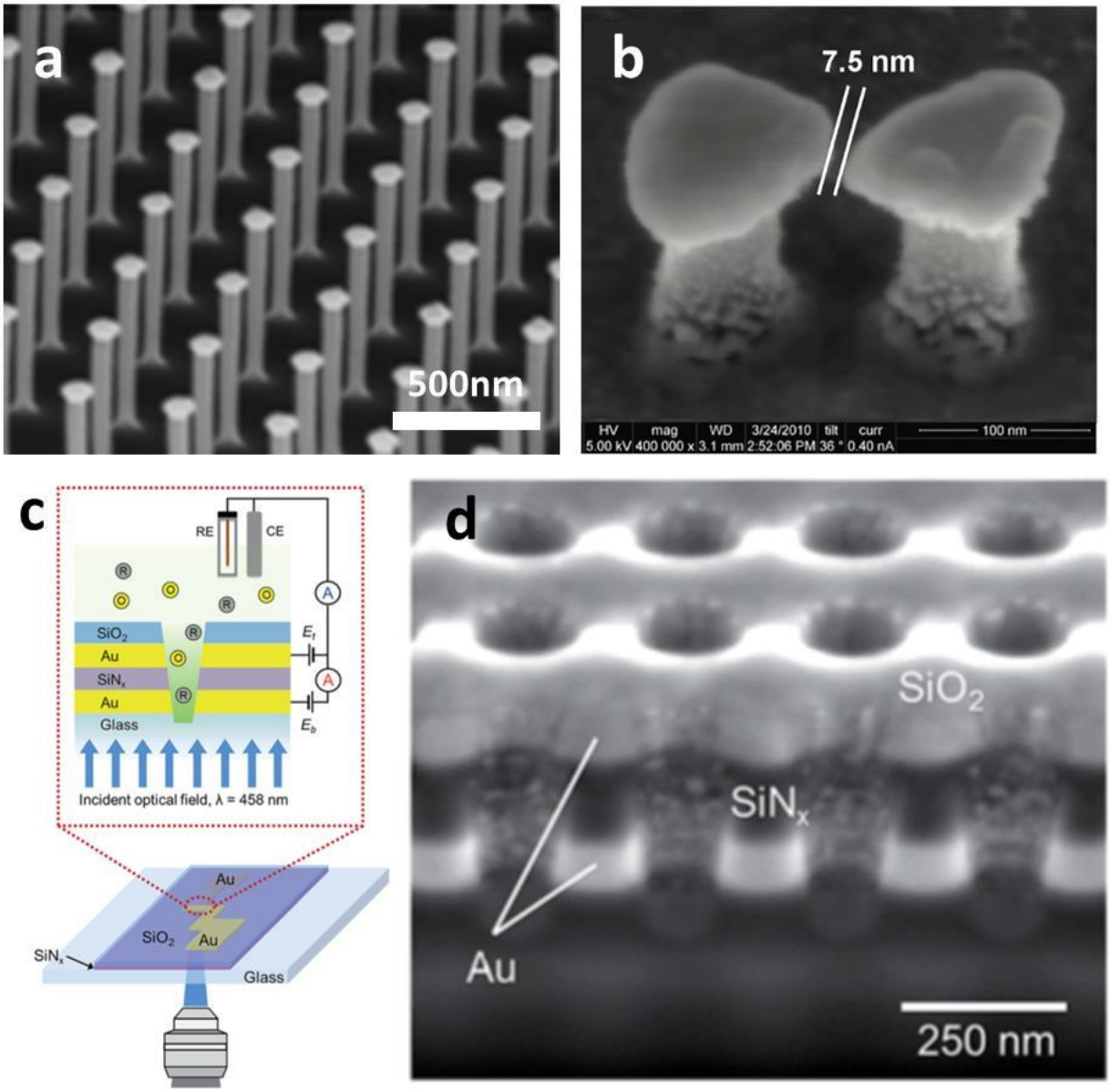
a
500nm
b
7.5 nm
HV mag WD 3/24/2010 tilt curr 100 nm
5.00 kV 400 000 x 3.1 mm 2:52:06 PM 36 ° 0.40 nA
c
RE
CE
A
SiO2
Au
SiNx
Au
Glass
E1
Eb
Incident optical field, λ = 458 nm
Au
SiO2
Au
SiNx
Glass
d
SiO2
SiNx
Au
250 nm